

Chapter 19

Studies of the Molecular Interaction Between Cellulose and Lignin as a Model for the Hierarchical Structure of Wood

Wolfgang G. Glasser, Timothy G. Rials¹, Stephen S. Kelley², and Vipul Dave³

Biobased Materials/Recycling Center and Department of Wood Science and Forest Products, Virginia Polytechnic Institute and State University, Blacksburg, VA 24061

Wood and dietary fiber products all belong to a class of **biomolecular** composites that are rich in cellulose and lignin. The interaction between cellulose and lignin determines such properties as mechanical strength (wood); creep, durability and aging; cellulose purity (pulp); and digestibility (nutrients). The understanding of the interaction between cellulose and lignin can be approached from various types of analyses involving the natural biocomposites, or it can be explored by studying the physical mixtures of the two types of macromolecules. The latter can be prepared by mixing the respective polymers in solid, solution or melt form within the constraints of **solubility** and melt-flowability. Such mixtures have been examined, and the results suggest that cellulose and its derivatives form two distinct phases with lignin and its derivatives; a crystalline polysaccharide-phase and a continuous amorphous phase that provides evidence for strong intermolecular interaction between the two components. In addition, results suggest that lignin and/or its derivatives are capable of contributing to the supermolecular organization of cellulose (derivatives). The interaction between lignin and cellulose varies in relation to chemical **differences** as well as molecular parameters. The results are consistent with the view that the hierarchical structure of the natural biocomposite wood is not only the consequence of a sequence of biochemical events, but

¹Southern Forest Experiment Station, U.S. Forest Service, Pineville, LA 71359

²National Renewable Energy Laboratory, Golden, CO 80401

³Johnson and Johnson, **Skillman**, NJ 08558

that it is the result of various thermodynamic driving forces that are independent of the biosynthetic origin.

Hierarchical structures “are assemblages of molecular units or their aggregates that are embedded or intertwined with other phases, which in turn are similarly organized at increasing size levels” (1). It is the multimolecular combination of virtually all biological materials that is responsible for the multilevel architectures that confer the unique properties to the composites of nature. Wood (or more generically, “lignocellulose”) is a complex material on all dimensional levels of the structural hierarchy, from the nano- to the millimeter-scale. Lignocelluloses are mixtures of crystalline and non-crystalline polysaccharides with lignin that are assembled into a structural architecture in which the interaction between the biomacromolecules is dictated by the specific sequence of biochemical events that take place during biosynthesis (i.e., plant growth). The resulting multilevel architecture determines all properties, regardless of whether these are mechanical, chemical, sorptive, nutritive, **rheological**, or degradative in nature. The understanding of hierarchical molecular structures in biological systems is beginning to be taken as a guide for the development of new, man-made materials (1). Several models have been advanced that describe wood (and lignocellulose) as a multiphase material that achieves its remarkable fracture toughness on the basis of the need to create an almost infinitesimal new surface area during **fracture** (2). It is the creation of **interfibrillar** cracks during mechanical failure which prevents **fiber** pullout at all levels of moisture sorption or temperature (2).

Single-phase materials, uniform polymers, often suffer **from** low impact strength and low dimensional stability when heated. New material properties are achieved when two or more types of molecules are blended or mixed. The resulting morphology of these mixtures is a direct result of the method of blending and the specific chemical **and** molecular interactions (3). Impact strength and resistance to deformation at elevated temperature rise when mixtures of macromolecules with distinct phases remain molecularly intertwined.

This paper reviews and **summarizes** a series of experiments designed to explore the specific molecular interactions between cellulose and **lignin** and their respective derivatives. Man-made blends of these biopolymers are to be compared with the natural biocomposite with a view towards determining the nature of the interaction between the two components. While it is evident that these interactions are also operative during the process of wood formation (i.e., **lignification**), between lignin precursors and the **polysaccharidic** matrix this paper is limited to **polymer-polymer** interaction **arguments**, exclusively. However, the reader is referred to the vast body of literature **dealing** with the biosynthetic aspects of the creation of molecular interactions between polysaccharides and **lignin**, such as the recent book by Jung et al. (4).

Experimental Section

Materials: All cellulose and cellulose derivatives were obtained as chemically pure, commercially available materials. **Lignin** and lignin derivatives were obtained from Aldrich Chemical Company except for derivatives described in the primary literature as indicated. Solvents were used as provided from chemical suppliers.

Methods: 1. **Blends:** Blends of cellulose with lignin were prepared by mixing cellulose solutions in **DMAc/LiCl** with lignin dissolved in **DMAc** in accordance with earlier work (5-10). Cellulose derivatives, hydroxypropyl cellulose, ethyl cellulose and cellulose mixed esters (CAB), were blended with lignin by using both melt and solution mixing. Common solvents were pyridine, dioxan and acetone. This work has been described in detail elsewhere (5-7). Melt-blended specimens were produced by injection molding.

2. **Thermal Analysis:** Thermal analysis was conducted using differential scanning calorimetry (**DSC**) and/or dynamic mechanical thermal analysis (DMTA) with either thin films (from solvent casting) or melt processed test specimens (dog bones from injection molding).

3. **Other Characterization Methods:** Ultimate strength was determined by tensile tests using an **Instron** tensile tester. Dynamic viscosity was determined on a Rheometrics Mechanical Spectrometer (**RMS 800**) using 20% (w/w) solutions in a parallel-disk geometry (10). Transmission electron microscopy was conducted on a Jeol SEM-IOOCX-II electron microscope. All methods have been described before where indicated.

Results and Discussion

L Wood

The non-crystalline component of wood, which is responsible for the **viscoelastic** nature of this natural material, gives rise to a variety of responses during heating (11-13). Whereas only a single, broad transition can be detected for native wood at low moisture content, a distinctly **trimodal** distribution of damping transitions ($\tan \delta$ peaks) can be detected at elevated moisture content (Figure 1). Whereas one transition (β) has no discernible impact on the storage modulus, and **can** safely be attributed to local site exchange of moisture, the **occurrence** of two distinct glass transition temperatures at which mechanical damping occurs suggests the existence of two different non-crystalline molecular entities. These undergo separate and independent glass to rubber transitions. Specifically, the existence of distinct $\tan \delta$ transitions in moist wood, at 30% moisture content, at **-10°C (α_2)** and **60°C (α_1)** (11), suggests the presence of two different molecular components that each reside in their independent phase on the molecular (**nano-**) level. By investigating the moisture response of these two glass transitions, and by

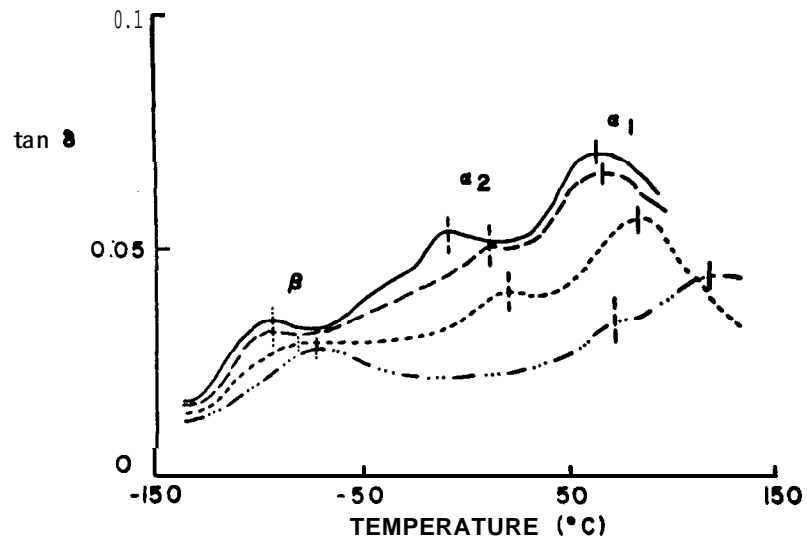


Fig. 1. DMTA spectra (tan δ -transitions) of a section of solid spruce wood recorded at moisture contents rising from 5% (bottom) to 10, 20, and 30% (top). Peaks α_1 , α_2 , and β reflect large-scale segmental motion and a secondary dispersion (p-transition) characteristic of glass transitions and site exchange of water, respectively. The T_g s were assigned to hemicelluloses (α_2) and lignin (α_1). According to ref. 11.

comparing them to isolated lignin preparations using the model of Kwei (14), α_1 and α_2 were attributed to the presence of the molecular phases representing lignin and hemicelluloses, respectively(11). However, it needs to be pointed out that the existence of separate phases as indicated by DMTA is not inconsistent with the existence of primary or secondary bonds between those phases. Block copolymers between thermoplastic cellulose derivatives and lignin were also found to exhibit phase distinctions with the individual blocks having molecular weights as low as 10^3 daltons (15, 16) There is strong evidence suggesting that the **two** non-crystalline components of wood, hemicellulose and lignin, are **covalently** linked in block copolymer fashion (17) and each of these two polymeric phases undergo an independent glass to rubber transition at a different temperature. Due to the hydrophilic nature of these phases, their transition temperatures depend on moisture content; and so does our ability to observe these transitions.

II. Cellulose Derivative/Lignin Blends

Any attempt at recreating wood's native structure by solvent or melt processes is complicated by the variability of the chemical structure of the matrix and the intractability of the cellulose in terms of solubility and melt properties. This limitation may be overcome in part by chemical modification in the form of derivatives. While it is recognized that this severely constrains the realism of the model, it does provide insight into the chemical and physical interaction that can be formed in a binary blend of lignin and cellulose derivatives.

The state of miscibility of a polymer pair is commonly evaluated by studying **T_g -behavior** in relation to the volume fraction of the respective polymers. Phase-separated mixtures exhibit the **T_g s** of the individual parent homopolymers while a single transition intermediate to the values of the individual homopolymers indicates miscibility. Partial miscibility is indicated by the **T_g s** migrating towards a single, common transition in relation to **fractional** mixing. The DSC-thermograms of a series of hydroxypropyl cellulose (**HPC**)/**lignin (L)** blends (prepared by injection molding) provide evidence for strong intermolecular interaction (Fig. 2) (5). A single **T_g** is observed for blends with a lignin content of up to **55%**, and this **T_g** rises with lignin content.

Dynamic mechanical thermal analysis (DMTA) of this same series of **HPC/L** blends (Fig. 3) reveals a similar elevation in temperature of damping transitions with lignin content rising. The two **tan δ** transitions of the pure **HPC**-spectrum (at 30 and **85°C**) have been assigned to the **T_g s** of an amorphous phase and that of an organized, liquid crystalline (**LC**) mesophase, respectively (18). The effect of lignin causes a **significant** reduction of the temperature range over which the **tan δ** transition occurs, with an apparent L-association with the LC mesophase to the exclusion of the lower-temperature amorphous phase (5). This behavior is in conflict with the normal effect of multiphase materials on thermal transitions (19). Normally, the glass to rubber transitions of a mixture of two non-crystalline

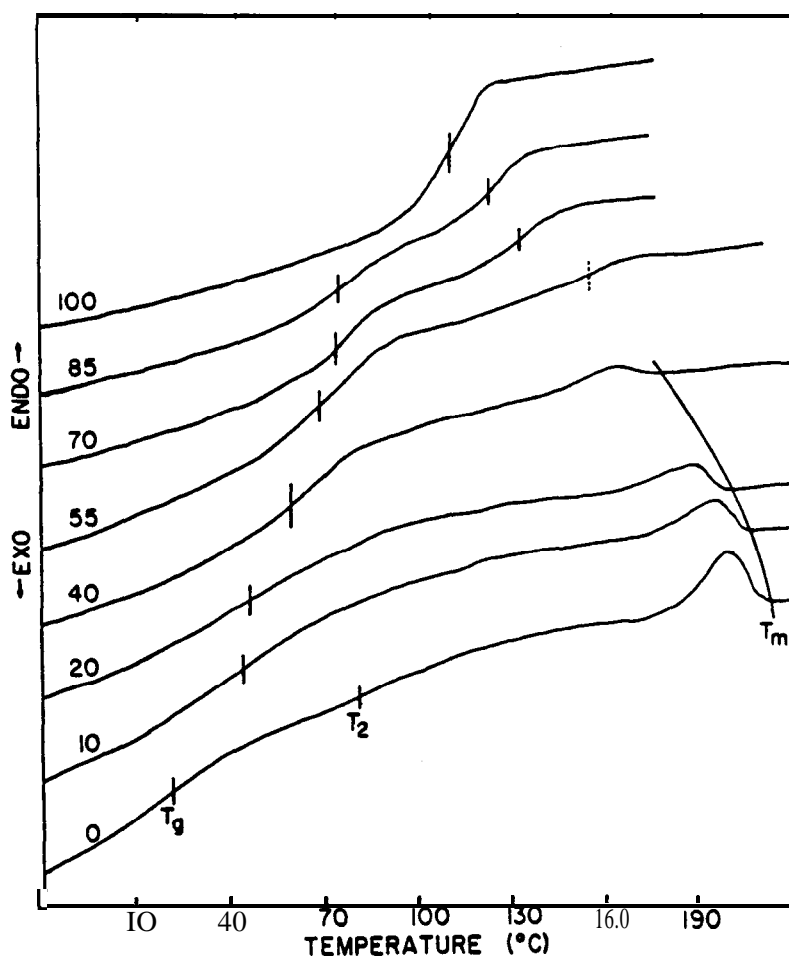


Fig. 2. DSC thermograms of solvent-cast films consisting of mixtures of hydroxypropyl cellulose (HPC) and organosolv lignin (L). Lignin content as indicated by the numbers of each tracing (0 to 100%). Both T_g and T_m show variation in relation to blend composition. T_2 has been attributed to a liquid crystalline mesophase present in HPC (18). According to ref. 5.

polymers broaden on the temperature-scale, and they may stretch over the entire region in which the constitutive components undergo thermal transitions in pure state if they are partially miscible. In the 55% L-content blend, a material with more highly ordered morphology is indicated (Fig. 3). The addition of lignin apparently contributes to the enhancement of HPC's LC mesophase at the expense of an amorphous phase.

A similar rise in relaxation intensity and simultaneous decrease in breadth of the tan δ transition was observed in blends of HPC with a partially ethylated lignin (EL) (Fig. 4) (6). However, in this case the improved uniformity of phase response results in the complete disruption of the super-molecular structure of the HPC and the formation of a seemingly continuous, miscible, amorphous blend of HPC and EL.

Different observations are made with blends of ethyl cellulose (EC) and L where the addition of a second, immiscible molecular component produces the expected broadening of the tan δ transition (Fig. 5) (7). Since the resulting two T_g -transitions, however, are found at temperatures below and above those of the respective parent (pure) components, the appearance of two separate phases is explained with the formation of a supermolecularly ordered (discrete) phase with a T_g above that of either parent constituent in addition to a lower- T , (uniform) amorphous phase. The creation of an LC mesophase architecture by the addition of lignin is also supported by an increase in storage modulus upon passage through T_g (not shown, refer to ref. 7).

An examination of the melting point of the HPC component in relation to lignin content revealed (5) that T_m migrates in relation to the volume fraction of lignin. The degree of melting point depression was approximately dependent on lignin volume fraction and a polymer-polymer interaction parameter, B (20). For blends with components whose molecular weight is $>2,000$, the melting point depression is approximately related to B according to

$$T_{m2}^0 - T_{m2} = \frac{-BV_{2u}}{\Delta H_{2u}} T_{m2}^0 \phi_1^2 \quad (1)$$

where the subscript 2 refers to the crystallizable component (i.e., HPC). T_{m2}^0 is its equilibrium melting temperature, $\Delta H_{2u}/V_{2u}$ is its heat of fusion per unit volume of repeat unit for 100% crystalline material, V_2 is its molar volume, and ϕ_1 is its volume fraction in the blend. B can be directly evaluated from the slope of a plot of $(T_{m2}^0 - T_{m2})$ vs. ϕ_1^2 (Fig. 6) (21). Working with lignin derivatives in which hydroxyl groups were selectively removed (by acetylation or ethylation), a relationship between B and the phenolic hydroxyl content was established (6). The interaction parameter was lowest (and intermolecular interaction most favorable) when the phenolic hydroxyl content was approximately 0.25 per phenylpropane repeat unit

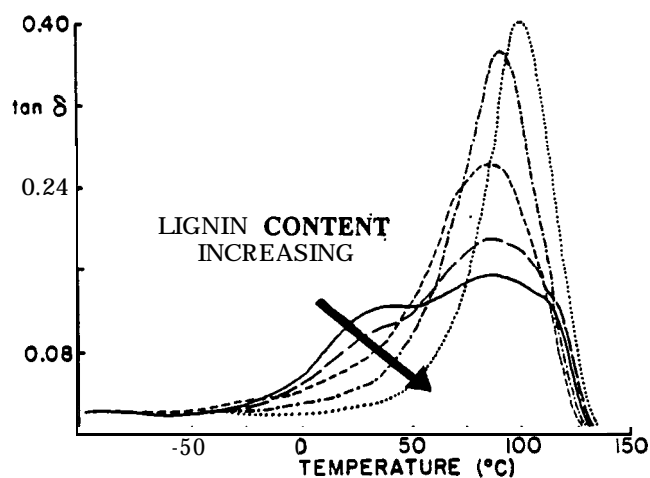


Fig. 3. DMTA Spectra (tan δ & transitions) of melt-processed **HPC/L** blends containing, 0 (-), 5 (--), 20 (---), 40 (-.-.-), and 55% (.....) L-content. The narrowing of the tan δ peak with rising L-content suggests an increasing degree of molecular interaction (According to ref. 5).

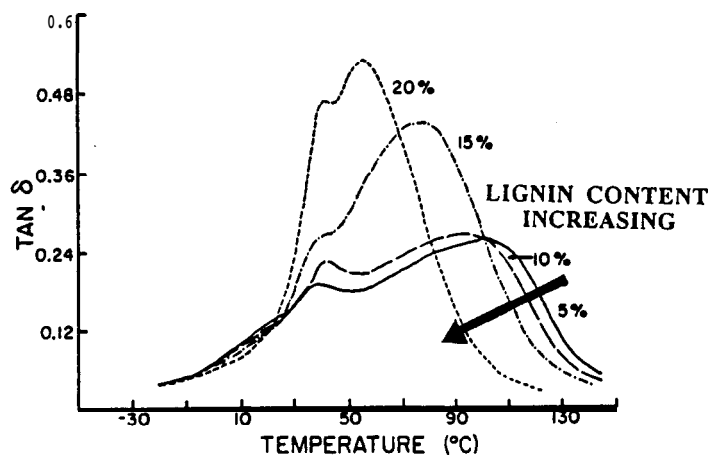


Fig. 4. DMTA spectra (tan δ & transitions) of solvent-cast blend films (dioxan) of **HPC** with ethyl lignin (EL). EL-content is indicated by the numbers of each tracing (5 to 20%). The progressive narrowing of the tan δ peak with rising EL-content suggests enhanced molecular interaction with L-content rising. According to ref. 6.

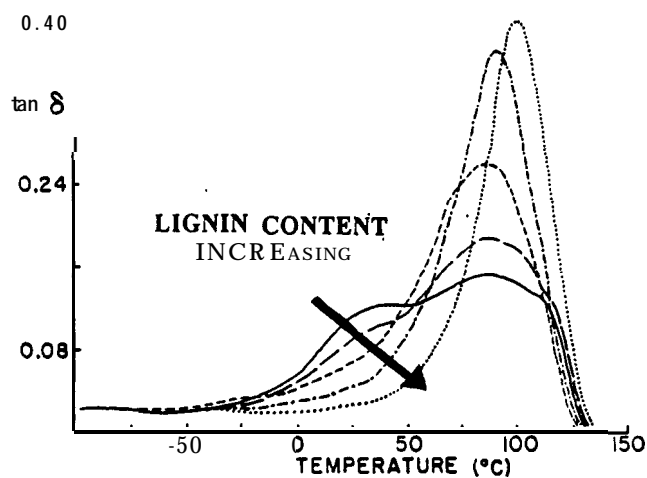


Fig. 3. DMTA Spectra ($\tan \delta$ -transitions) of melt-processed HPC/L blends containing, 0 (-), 5 (--), 20 (---), 40 (-.-.-), and 55% (.....) L-content. The narrowing of the $\tan \delta$ -peak with rising L-content suggests an increasing degree of molecular interaction (According to ref. 5).

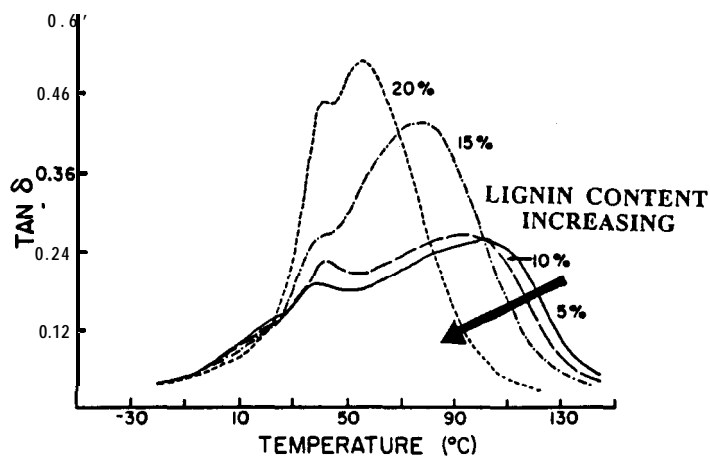


Fig. 4. DMTA spectra ($\tan \delta$ -transitions) of solvent-cast blend films (dioxan) of HPC with ethyl lignin (EL). EL-content is indicated by the numbers of each tracing (5 to 20%). The progressive narrowing of the $\tan \delta$ -peak with rising EL-content suggests enhanced molecular interaction with L-content rising. According to ref. 6.

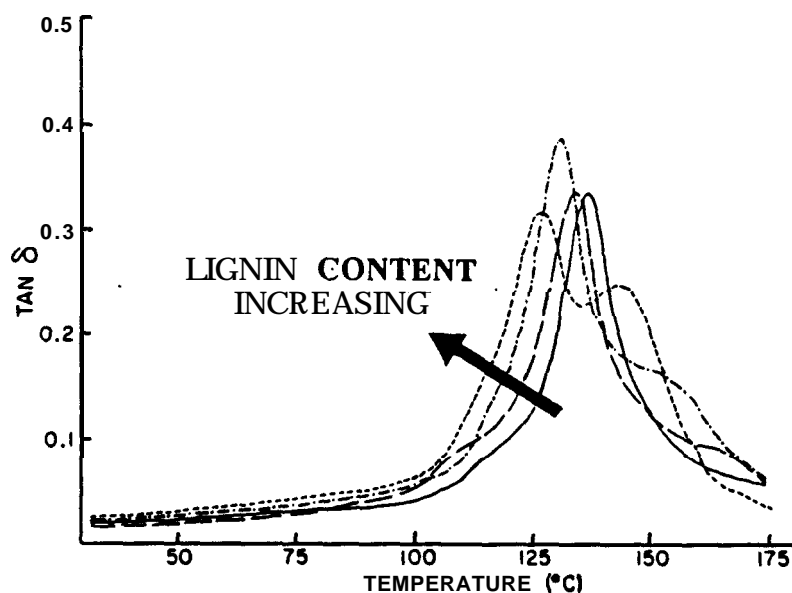


Fig. 5. DMTA spectra (tan & transitions) of solvent-cast blend films (dioxan) of ethyl cellulose (EC) with organosolv lignin(L). L-content rises from 0 (--) to 10 (---), 20 (-.-), and 40% (-.-.-). The separation of the tan & peak into two distinct transitions is as expected for a **molecularly** immiscible blend; however, since the higher-temperature transition (at ca 147°C) is higher than the two parent polymer components, this is attributed to a supermolecularly-ordered phase that is separated **from** a uniform (continuous) amorphous phase. (Lignin- T_g is at 95°C). According to ref. 7.

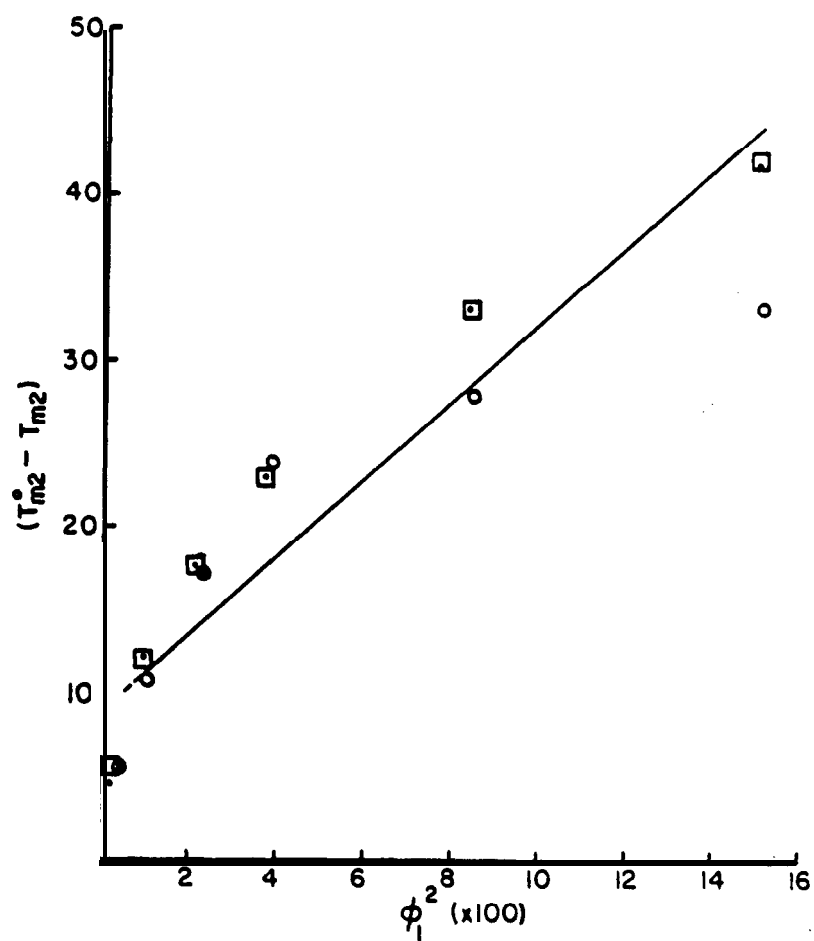


Fig. 6. Relationship between $(T_{m2}^{\circ} - T_{m2})$ and ϕ_1^2 from eq. 1 for HPC/L blends prepared from dioxan (O), pyridine (●), and from melt (□). According to ref. 5.

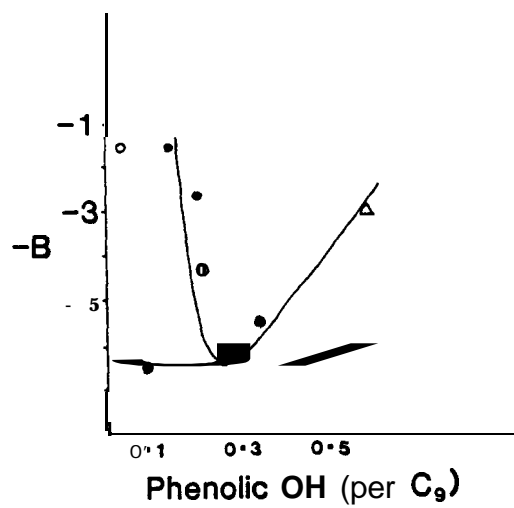


Fig. 7. Relationship between polymer-polymer interaction parameter, B , and a lignin structural feature (i.e., phenolic OH-content per C_9 -repeat unit). The lowest value for B denotes greatest interaction between polymers. According to ref. 6.

in lignin (Fig. 7). This indicates that the **lignin** which has a structure (in terms of functionality) similar to the one in native wood, is the one that provides for conditions most favorable to strong intermolecular interaction between cellulose (derivatives) and lignin, and this favors component miscibility (5-7).

In an attempt to **further** increase the phase compatibility between lignin and cellulose (derivatives), block copolymers were synthesized which consisted of covalently-linked lignin and cellulose ester segments (or "blocks") (15-16). It was revealed that copolymer architecture, which normally enhances phase compatibility, was unable to provide further improvements in **lignin/cellulose** (derivative) blend compatibility (16). Glass transition temperatures were shifted towards an intermediate temperature for low molecular weight copolymers, but they did not migrate for high molecular weight components, when blended with cellulose propionate (CP) regardless of whether the lignin was the component of a **lignin-CP** block copolymer or not (not shown, refer to ref. 16). No improvement in miscibility resulted **from** the modification of lignin by **copolymerization** with CP segments.

The blend experiments involving cellulose derivatives and lignin suggest that lignin disrupts both the ordered and the non-ordered forms of cellulose derivative morphology by favoring the formation of an amorphous or liquid crystalline mesophase structure through strong interactive association between lignin and the **polysaccharide** component.

III Regenerated Fibers

The spinning of cellulose **from** an ordered solution state has become commercial practice with the introduction of an N-methyl **morpholine-N-oxide**-based solvent process (22). Cellulose *ester* derivatives can also be converted into fibers by spinning **from** an anisotropic, liquid crystalline solution-state in a variety of solvents (10, 23-26). The formation of anisotropic solutions of cellulose esters in various solvents has been studied in detail (27). Continuous cellulose ester fibers were found to exhibit the expected behavior in terms of mechanical (tensile) properties (i.e., increased strength with **increasing** orientation) when spun **from** biphasic or anisotropic solutions (24). The addition of lignin to cellulose and cellulose ester solutions was found to impact the dynamic elastic modulus of concentrated solutions differently: whereas the addition of lignin reduced the dynamic elastic modulus of cellulose ester solutions at all levels of lignin content, cellulose solutions (**in DMAc/LiCl**) became more viscous (Fig. 8). Considering that isolated lignin has a molecular weight of only ca **1/100th** that of cellulose and cellulose esters, and lignin is usually considered to be a highly compact or spherical molecule, its impact was expected to be one of viscosity-reduction. The fact that the dynamic elastic modulus of cellulose, but not of cellulose ester, solutions increased instead to decline at all shear frequencies is explained with strong secondary interactions of lignin with cellulose in the **DMAc/LiCl** solvent system.

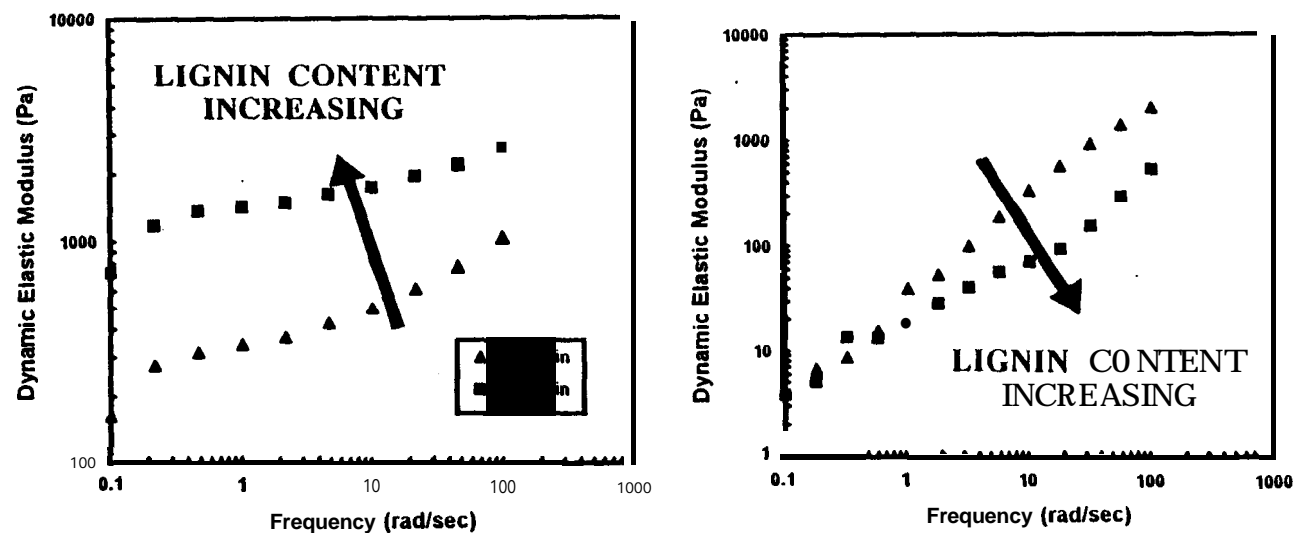


Fig. 8. The dynamic elastic modulus of cellulose(**left**) and cellulose ester (CAB) (**right**) solutions with lignin **in DMAc** (with **LiCl** added in case of cellulose), in relation to lignin content at different frequencies. Whereas the presence of lignin in the solution raises the modulus of the **cellulose/lignin** mixture at all frequencies, lignin contributes to a reduction of solution modulus at all **frequencies** in case of cellulose esters. According **tref.10**.

However, even when cellulose ester (cellulose acetate butyrate **CAB**)/**L** mixtures were spun into continuous fibers from **DMAC** solution, both fiber tensile strength and modulus increased significantly (10). The strength and modulus (**stiffness**)-enhancing effect of lignin on cellulose ester fibers was limited to the initial 4%; beyond 4% lignin content, no further positive effect of lignin on fiber strength was noted (Figure 9). It is surprising that the addition of small amounts of (low molecular weight, isolated) lignin neither interfered with the formation of anisotropic solutions nor with the ultimate strength of the resulting fibers (10). A tenacity-increasing effect of small amounts of lignin on cellulose ester fibers can be explained only with a positive effect by lignin on the molecular order of the cellulose derivative in solution and in solid state (10).

The propensity of cellulose esters to form liquid crystalline morphologies has been observed previously (27). A recent study has indicated that the addition of lignin enhances the formation of ordered structures in cellulose acetate butyrate (**CAB**) (28). Experimental evidence suggests that, as solvent evaporates and both constituents solidify, the surface of phase-separated lignin particles serves to create **cholesteric** liquid crystalline order by nucleation (Figure 10) (28). The resulting structure provides evidence that lignin phase-separates **from** cellulose ester derivatives and becomes an integral part of a two-phase architecture in which the degree of organization in the polysaccharidic matrix is substantially increased at the apparent expense of an amorphous phase. The addition of lignin was consistently found to enhance the liquid crystalline mesophase order in non-crystalline cellulose derivatives, and this order is **often** responsible for increased strength properties. A similar phase-separated morphology also was found in blends of cellulose with lignin (Fig. 11). This morphology reveals heterogeneity at the **nano-level**, and this provides the basis for a structural hierarchy that has become the trademark of biological materials, such as wood (1).

CONCLUSIONS

Results with blends of cellulose and cellulose derivatives with lignin suggest that the two biopolymers are immiscible.

Experimental evidence supports the hypothesis that lignin enhances the organization of non-crystalline cellulosic structures and gels, and that liquid crystalline mesophase, ordered structures are created that result in multiphase architectures. This enhanced heterogeneity **often** produces materials with higher modulus and higher strength.

The effect of lignin in blends with cellulose esters is found to disrupt both crystalline order and non-crystallinity by contributing to the formation of a mesophase liquid crystalline morphology that produces an architecture on the dimension of nanometers. This secondary order is held responsible for observed strength gains in **lignin/cellulose** derivative blends.

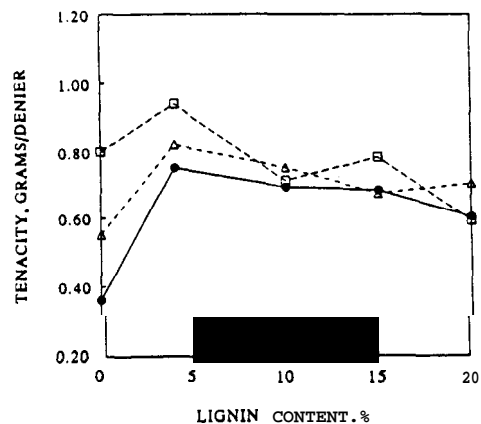


Fig. 9 Relationship between CAB-fiber tensile strength and lignin content at different draw ratios. (Draw ratios increase from 0.8, -●-, to 1.5, -□-, for all lignin contents except 20%, where they ranged between 0.26 and 0.5, respectively.) Tensile strength is seen to increase with lignin content rising to 20%. This is unexpected since lignin has a molecular weight of only ca 1/100th of that of cellulose derivative and is expected to reduce tensile strength in relation to degree of dilution. According to ref. 10.



Fig. 10. Transmission electron micrograph (TEM) of a cellulose ester (CAB) film containing 20% lignin. The unstained film shows a phase-separated particle that provides a nucleating surface for cellulose ester liquid crystals. The well-ordered cholesteric arrangement was found to be distinctly more pronounced in the presence of lignin. The periodicity between striation lines was smallest on the surface of the lignin particle indicating lignin's contribution to the cellulose ester's organization. According to ref. 28.

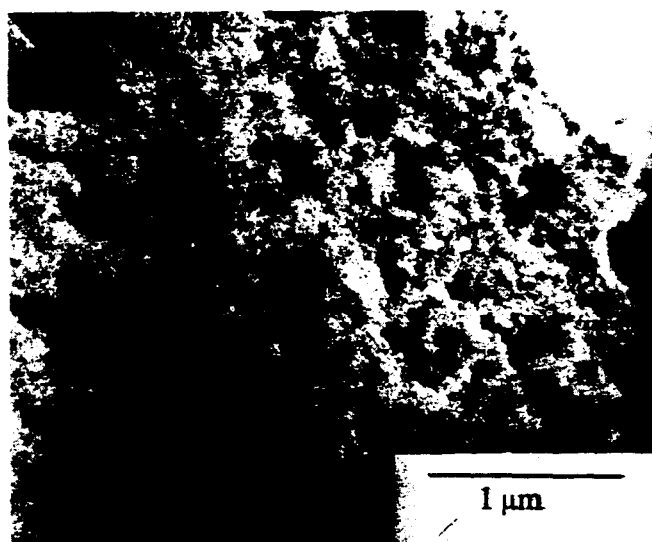


Fig. 11. Transmission electron micrograph (TEM) of the stained cross-section of a cellulose/lignin blend fiber containing 4% (w/w) lignin. There is evidence for an even dispersion of lignin particles in the size-range of 10-20 nm in addition to much larger aggregates.

The results suggest that the natural composite structure of **lignified** plant materials is not only a consequence of a sequence of well-defined biochemical events, but that it is also a consequence of the thermodynamic driving forces that regulate the interaction between the most prevalent polymer constituents present in **lignocellulose**, **lignin** and (**cellulosic**) polysaccharides.

ACKNOWLEDGMENTS

This report is based on studies financially supported by the National Science Foundation (Washington, D.C.), the Center for Innovative Technology (**Herndon**, VA), and the USDA (Washington, DC).

LITERATURE CITED

1. National Research Council, "Hierarchical Structures in Biology as a Guide for New Materials Technology," National Materials Advisory Board, ed., National Academy Press, Washington, DC, 1994; pg. 1.
2. G. Jeronimidis, "Wood, One of Nature's Challenging Composites," in "The Mechanical Properties of Biological Materials," SEB Symposium No. 34, Cambridge Univ. Press, Cambridge, England, 1980, 169-182.
3. T. A. Oswald and G. Menges, "Materials Science of Polymers for Engineers,* Hanser Publishers, Munich **Vienna New York**, 1995,475 pg.
4. H. G. Jung, D. R. Buxton, R D. Hatfield, and J. Ralph, editors. "Forage Cell Wall Structure and Digestibility," American Society of Agronomy, Inc., Madison, **Wisc.**, 1993; 794 pg.
5. T. G. **Rials**, W. G. Glasser, J. Appl. Polym. Sci**37**, **2399-2415** (1989).
6. T. G. Rials, W. G. Glasser. Polymer 31, 1333-1338 (1990).
7. T. G. Rials, W. G. Glasser, Wood and Fiber **Sci.21(1)**,**80-90** (1989).
8. V. J. H. **Sewalt**, W. de Oliveira, W. G. Glasser. J. Sci. Food Agric. 71, 204-208 (1996).
9. **G. Gamier**, W. G. Glasser, Polymer Eng. Sci. **36**, **885-894** (1996).
10. **V. Davé**, W. G. Glasser, Polymer**38**, **2121-2126** (1997).
11. S. S. Kelley, T. G. Rials, W. G. Glasser. J. Mater. Sci. 22,617 (1987).
12. L. **Salmen**, J. Mater. Sci.**19**, **3090** (1984).
13. A.-M. **Olsson**, **L-Salmén**, Chapter 9 in "Viscoelasticity of Biomaterials," W. Glasser and H. **Hatakeyama**, eds., ACS **Symp.** Ser. 489, 133-143 (1992).
14. T. K. Kwei, J. Polym. Sci.: Polym. Lett. 22,307 (1984).
15. W. de **Oliveira**, W. G. Glasser. Macromolecules 27. **5(1994)**.
16. W. de **Oliveira**, W. G. Glasser. Polymer **35(9)**, 1977-1985 (1994).
17. N. **Terashima**, K. **Fukushima**, L.-F. He, K. Takabe. Chapter 10 "Comprehensive Model of the Lignified Plant Cell **Wall**," in "Forage Cell Wall Structure and Digestibility," H. G. Sung, D. R. Buxton, R D. **Hatfield**,

- J. Ralph, Eds., Amer. Soc. Agronomy, Inc., Madison, Wisc., 247-270 (1993).
18. T. G. Rials, W. G. Glasser, J. Appl. Polym. Sci. **36**, 749-758 (1988).
 19. E. A. Turi, ed. "Thermal Characterization of Polymeric Materials," Academic Press, New York 1981, 972 pg.
 20. P. J. Flory. J. Chem. Phys. 17, 223 (1949).
 21. J. E. Harris, D. R. Paul, J. W. Barlow. In "Polymer Blends and Composites in Multiphase Systems," ACS Adv. Chem. Ser., No. 206, C. D. Han, ed., 1984, 17.
 22. S. A. Mot-timer, A A Peguy, Cellulose Chem. Technol. 30, 117-132 (1996).
 23. V. Dave, W. G. Glasser. In "Viscoelasticity of Biomaterials," W. G. Glasser and Hatakeyama, eds., ACS Symp. Ser. No. **489**, 144-165 (1992).
 24. V. Dave, W. G. Glasser, G. L. Wilkes. J. Polymer Sci., Pt. B: Physics, 31, 1145 (1993).
 25. V. Dave, W. G. Glasser. J. Appl. Polym. Sci. 48, 683 (1993).
 26. V. Dave, J. Wang, W. G. Glasser, D. Dillard. J. Polym. Sci., Pt. B: Physics 32, 1105 (1994).
 27. P. Zugenmaier, J. Appl. Polym. Sci.: Appl. Polym. Symp. 37, 223-238 (1983).
 28. V. Dave, W. G. Glasser, G. L. Wilkes. Polymer Bulletin 29, 565-570 (1992).
 29. J. R Penacchia, E. M. Pearce, T. K. Kwei; B. J. Bulkia, J.-P. Chen, Macromolecules 19, 973 (1986).

A C S S Y M P O S I U M S E R I E S **688**

Cellulose Derivatives

Modification, Characterization, and Nanostructures

Thomas J. Heinze, EDITOR
Friedrich-Schiller-Universität Jena

Wolfgang G. Glasser, EDITOR
Virginia Polytechnic Institute and State University

Developed from a symposium sponsored by the Division
of Cellulose, Paper, and Textiles at the 212th National Meeting
of the American Chemical Society,
Orlando, Florida,
August 25-29, 1996



American Chemical Society, Washington, D.C.